

Tensile and Fracture Toughness behavior of Centrifugally Cast Al/Al₂O₃ Functionally Graded Materials

Bhupendra Kumar^{a,b}, Amit Joshi^{*a}, Krishan Kant Singh Mer^{ab}, Lalta Prasad^c, & Indradeep Kumar^d

^aGovind Ballabh Pant Institute of Engineering and Technology, Pauri-Garhwal 246 194, India.

^bDepartment of Mechanical Engineering, Institute of Technology, Gopeshwar, Chamoli 246 401, India.

^cDepartment of Mechanical Engineering, National Institute of Technology Srinagar (Garhwal), Uttarakhand 246 174, India

^dDepartment of Aeronautical Engineering, Institute of Aeronautical Engineering, Hyderabad, Telangana 500 043, India

Received: 9 September 2022; Accepted: 17 October 2022

The mechanical characteristics like tensile strength and fracture toughness of aluminium-based functionally graded material (FGM) have been studied in the present work and correlated with the variation in the quantity of reinforcing particles. Aluminium based FGM with various compositions of reinforcing particles Al₂O₃ has been produced in the centrifugal casting set up rotating at a constant speed. The composition of reinforcing particles Al₂O₃ has varied from 3.0 to 7.5 Vol. %. ASTM standard has followed to prepare the samples for mechanical testing i.e. tensile and 3-point bend testing. Tensile strength and fracture toughness were calculated on each sample to study the deformation behaviour of Al alloy and FGM samples. A significant enhancement in the values of tensile and fracture measuring parameters has reported with an increase in % vol. of Al₂O₃ particles.

Keywords: Matrix Composite, Functionally Graded Materials, Scanning Electron Microscopy, Fracture Toughness, Tensile strength

1 Introduction

In current engineering applications, there is an inclination towards the incorporation of materials that are light in weight, strong and relatively economic materials. With the swift advancement of novel technologies, the necessity for such types of materials is also intensifying. To meet out this requirement, a combination of metals and monolithic reinforced materials (pre-existing) are widely explored and utilized. The addition of mono-lithic materials in the base composition augments the characteristics of combined material (i.e. composite material) and it reflects the exceptional properties which were not experienced in the base composition alone.

Usually, composite materials own two phases: the first one is the matrix i.e. the base composition comprising

60-90% of the composite, and the second one is the reinforcement i.e. the compound added in dissimilar proportions (small) to augment the characteristics of the matrix material. It implies that in composite material, matrix material consists of a small % of reinforced material by volume or weight^{1, 2}. Recent

advancements in engineering and materials processing have led to the novel class of materials namely 'functionally graded materials (FGMs)'. FGMs exemplifies the special class of composite materials and have been designed to attain extraordinary levels of performance³. FGMs become noteworthy to augment the mechanical as well as the tribological properties of composites by making the gradient transition zone in the middle of matrix and particle phases⁴. The concept of FGMs was considered first in 1984⁵ during a space plane project in Japan, where a mixture of the materials used was intended to offer a thermal barrier that can resist the surface temperatures of 1700°C and 700°C across a 10 mm thick⁶. The gradient is present continuously from one to other materials (gradient occurs continuously concerning a position in structure as well as in microstructure) in continuous grouping FGMs, whereas the gradient is present in a layered manner (microstructural characteristics changes in a gradual manner which results in multi-layer interface composition between discontinuous layers) in discreet grouping FGMs⁷.

In the past two decades, owing to the extensive technological as well as commercial significance of FGMs based Aluminium metal matrix composites

*Corresponding author (E-mail: amitj4765@gmail.com)

(MMCs) attracted the attention of scientists, technologists and intellectuals concerns⁸. The key benefits of FGM based Aluminium (Al) MMCs are their good resistance to heat, outstanding tribological and fatigue characteristics, extraordinary stiffness and weight strength⁹. Reinforcement in such materials can be done by the hard ceramic particles like B_4C , Al_2O_3 , TiC and SiC . A higher fraction of reinforcement in Al MMCs leads to the probability of breaking of material¹⁰. The rise in the weight of reinforcement particles in the Al matrix material makes Al MMCs brittle in nature¹¹. Many researchers studied increase or decrease the size of reinforcement particles to fabricate the MMCs, and analyzed the tensile and fracture behaviour of metal^{12, 13}.

In literature, the methods for producing FGMs include centrifugal casting¹⁴, powder metallurgy,¹⁵ vapor deposition,¹⁶ solid freeform (SFF) fabrication including additive manufacturing¹⁷. FGMs can be divided into two categories: the first one is the continuous grouping which includes the FGMs fabricated by methods like diffusion bonding and centrifugal casting, and the second one is a discreet grouping which includes the FGMs fabricated by methods like additive manufacturing and powder metallurgy^{18, 19}. The fabrication techniques such as powder metallurgy and centrifugal casting have proven effective in fabricating FGMs with the gradient in microstructures²⁰. Out of these two methods, the samples produced by the centrifugal casting method are larger as compared to the samples obtained by the powder metallurgy method which makes the centrifugal casting method more suitable for producing FGMs²¹. Another advantage of using centrifugal casting for the fabrication of FGMs includes the continuous distribution of particles within the matrix in a simple and cost-effective manner when compared to other fabrication methods²². This is the reason why functionally graded aluminum matrix composites (FGAMCs) has proven to be best suited for applications like the aerospace and automobile sector,²³ and further use with the development of centrifugal casting methods will be expected²⁴.

Recently, Ulukoy et. al.²⁵ investigated the mechanical characteristics of Al-based metal-matrix composite (MMC) with SiC reinforcement manufactured by centrifugal casting method. They observed that many SiC reinforcement particles were deposited in the outer space of the casted FGM cylinder during the casting process. They attributed

this deposition owing to the relatively higher density of reinforcing particles which in turn changes the mechanical characteristics across the cylinder diameter.

Ramasamy et al.²⁶ studied the influence of raster angle of ultimate tensile strength, the higher UTS has been obtained for the specimen built at raster angle of $0^\circ C$, penetrate infill pattern and evolved orientation of $45^\circ C$. Galy et. al.²⁷ studied the impact of $SiCp$ particles on mechanical characteristics of FGM. They machined the FGM samples in the form of tube and properties were measured along the whole thickness of the tube. They observed the enhanced value of tensile strength at the expense of ductility while increasing the weight fraction of reinforcement $SiCp$. They also monitored the UTS (ultimate-tensile strength) of FGM improves with the rise in fraction of reinforcing particulates (i.e. $SiCp$) and decrease with the diameter of particles. Saadatmand et al.²⁸ analyzed and modeled the monotonic strength of Al- SiC FGM and noted that the UTS of FGM depends on the number of layers and the mass fraction of SiC in the obtained sample. Guo et al.²⁹ studied the impact of the addition of nano- Al_2O_3 particles on the mechanical behavior of friction stir deformed (FSD) Al and reported the increased micro hardness and tensile properties of developed composite. The tensile characteristics of metal matrix composites were observed to be dependent on numerous microstructural features like grain-size of particles, dislocation content and interaction of reinforcing particle with base metal as described in their work. Zarghani et. al.³⁰ deliberated the microstructure and mechanical characteristics of FSD Al/ Al_2O_3 nano-composite and reported the improved hardness values and resistance to wear in nanocomposite owing to more uniform dispersal of nano-sized alumina particles with the rise in the number of FSD passes.

Based on the above studies it may be mentioned that to date most of the researchers have investigated the monotonic and tribological behavior of FGMs, however, fracture toughness evaluation in FGM prepared by centrifugal casting technique is limited in literature. Fracture toughness provides the diversified deformation behavior of metals/alloys. The fracture behavior in presence of pre-existing crack may be determined by performing fracture toughness tests. Fracture toughness evaluation in functionally graded material has been studied by very few researchers due to the difficulty in obtaining appropriate sample

dimensions, developing pre-existing cracks and presence of inherent defects which may cause unstable crack growth during fracture toughness testing.

Recently, Tohgo *et. al.*³¹ performed the 3-point bend test on an FGM and non-FGM sample containing partially-stabilized zirconia/austenitic-stainless steel fabricated by powder metallurgy. Their study revealed the higher value of fracture toughness in FGM samples due to stable crack growth as compared to non FGM samples where unstable crack growth was observed. Rousseau *et.al.*³² monitored the effect of crack location, crack length and crack kinking on the functionally graded material (FGM) and bi-materials. FGM samples have shown better failure performance as compared to bi-materials for all crack locations, crack length and crack kinking in their work. Apart from this most fracture toughness related investigations are based on the fracture toughness distribution and R-curve in growing mode I-crack³³⁻³⁶. However a detailed investigation on the evaluation of fracture toughness in FGM manufactured by stir-casting method is limited in the literature.

Therefore, this work examines the mechanical characteristics like tensile and fracture properties of Al MMC based FGM reinforced with Al₂O₃ particles. The mechanical properties are evaluated through tensile and fracture toughness tests and related with microstructure and fractography by using SEM.

2 Materials and Methods

In this work, Al 6061-O alloy was used as a matrix material and the composition for the same is provided in Table 1. The particles of Al₂O₃ with dissimilar volumetric fractions such as 3.0%, 4.5%, 6.0% & 7.5% were used as reinforcement having a mean grain size of 85 μm. The stir casting along with the centrifugal-casting technique was used to fabricate FGM. Firstly, with the help of the stir casting process a homogeneous metal matrix composite (MMC) were produced and then centrifugal-casting technique was adopted to manufacture the FGM.

Initially, the metal was melted in a pit furnace and then the reinforcement (Al₂O₃) was added homogeneously with the help of a stirrer in dissimilar volumetric percentages as shown in Figs 1(a-b). The pre-heating of cylindrical mould was done before pouring of prepared melted metal into it and rotated at a constant speed of 780 rpm. The schematic and actual diagram representing the same is displayed in Figs 1 (c-d). Further, the casting was exposed to room temperature for cooling.

The above procedure was replicated with dissimilar volume fractions of reinforcing Al₂O₃ particles to obtain the FGM in ring form (inner radii: 42 mm,

Table 1 — Al 6061-O alloy composition

Elements	Si	Fe	Mg	Cu	Mn
Percentage distribution	0.60	0.22	0.8	0.1	0.04

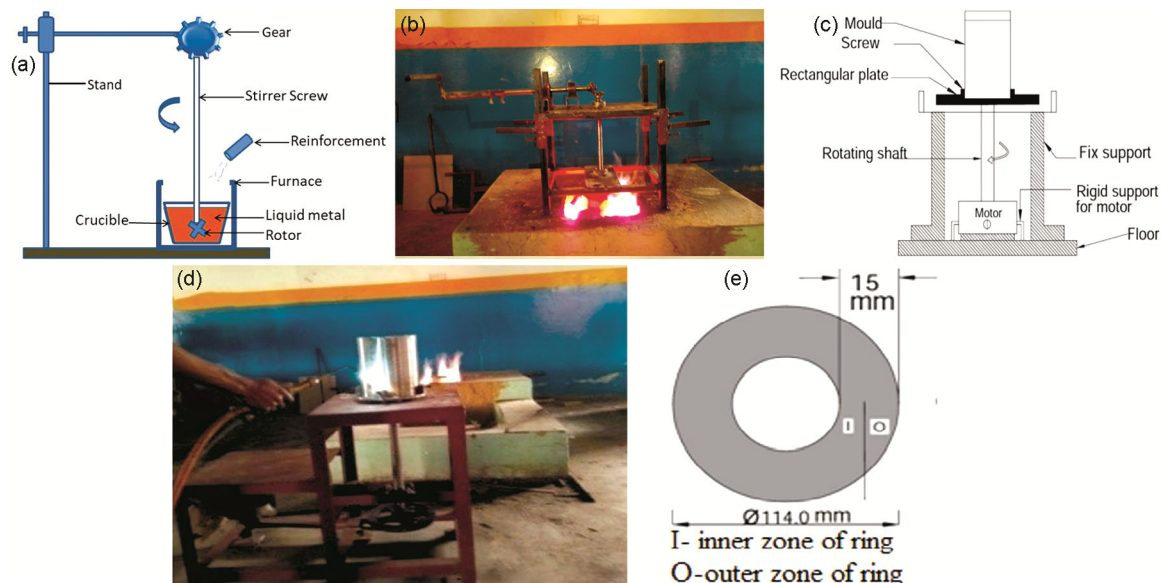


Fig. 1 — Various processes used: (a) line diagram of Stir-casting process, (b) experimental set-up for stir-casting process, (c) Line diagram of centrifugal casting machine, (d) pre-heating of centrifugal casting process, and (e) cross-sectional view of cast product.

thickness: 15 mm) as shown in Fig. 1(e). The FGM produced in ring form was then divided into different sections to make the samples for the tensile testing and fracture toughness testing. The mechanical testing was executed in room temperature conditions. ASTM: E8 sub-size specimen (having gauge length of 25 mm, width and thickness of 5 mm and 3 mm respectively) standard was used to prepare the sample for tensile testing while ASTM E399-05 standard³⁷ was used to prepare the samples for 3-point bend testing. Fig. 2 represents the typical dimensions of the sample for the 3-point bend test.

3 Results and Discussion

3.1 Microstructure

The SEM micrographs of the pure Al alloy and Al_2O_3 reinforced sample conditions are exhibited in the Figs 3(a-e). Fig. 3(a) depicts the microstructure of pure Al alloy sample and it can clearly be observed that there is no trace of reinforcing particle in it while for other sample conditions, the fraction of reinforcing particle Al_2O_3 can be observed clearly (Figs 3(b-e)). In these SEM micrographs, the percentage of reinforcing particles increases with a

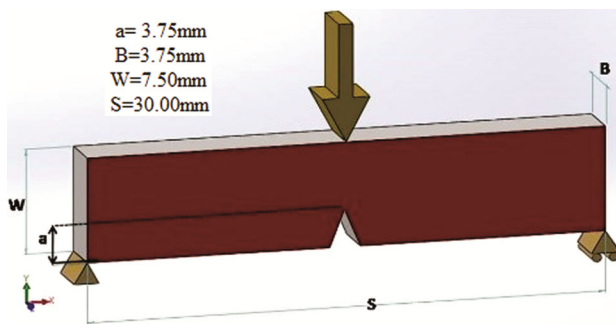


Fig. 2 — Specimen for 3- point bend test.

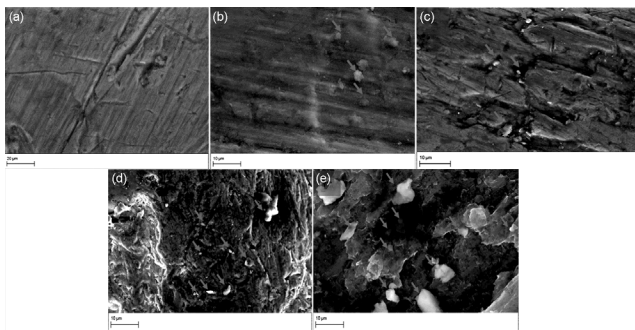


Fig. 3 — SEM images for (a) Pure Al-alloy, (b) Inner zone of 3.0 vol. of Al_2O_3 reinforcement, (c) Outer zone of 3.0 vol. of Al_2O_3 reinforcement, (d) Inner zone of 7.5% vol. of Al_2O_3 reinforcement, and (e) Outer zone of 7.5% vol. of Al_2O_3 reinforcement.

different volume percentage of Al_2O_3 reinforcement due to which area fraction of the postulates increased in inner as well as in outer zone (Figs 3(b-e))³⁸.

Figure 3(e) depicts that most of the Al_2O_3 particles in 7.5% vol. of Al metal matrix FGM are more in the outer zone of the cylinder while some Al_2O_3 particles congregated with lesser density and cumulate to the inner zone of the cylinder. This might be owing to the centrifugal force acting during the process of centrifugal casting. Similar observations were reported by Prasad et al.³⁹ during the investigation on the effect of reinforcing particles on microstructural characteristics of Al/ Al_2O_3 . Moreover, the inner zone provides a lesser area fraction of postulates as compared to the lesser reinforcing samples (3% vol.) in the outer zone. On the other hand, when the % content of reinforcing particles increases up to 7.5% vol., the smooth variation of particles was observed from inner-zone to outer-zone owing to low centrifugal speed as reported in the literature^{40, 41}.

3.2 Mechanical characteristics

Figures 4, 5, and Table. 2 shows the plot of the tensile strength (YS and UTS) and Vickers hardness for Al alloy and various FGMs samples with an increased percentage of reinforced starting from 3 to 7.5 % vol. The pure Al alloy possesses the yield strength (YS) of 34 MPa, ultimate tensile strength (UTS) of 58 MPa, Vickers hardness of 27.4 HV and ductility of 43%. The YS, UTS and hardness in FGMs sample reinforced at 3% vol. have boosted to 61.4 MPa, 87 MPa and 35.15 HV respectively, although the decrement in the ductility (21%) is observed in comparison to the pure Al alloy sample. This might be due to the null appearance of reinforcing particles in

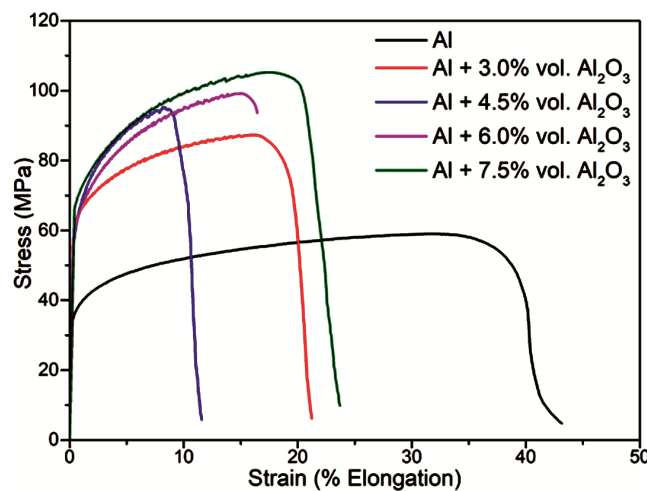


Fig. 4 — Stress strain curve for all material conditions.

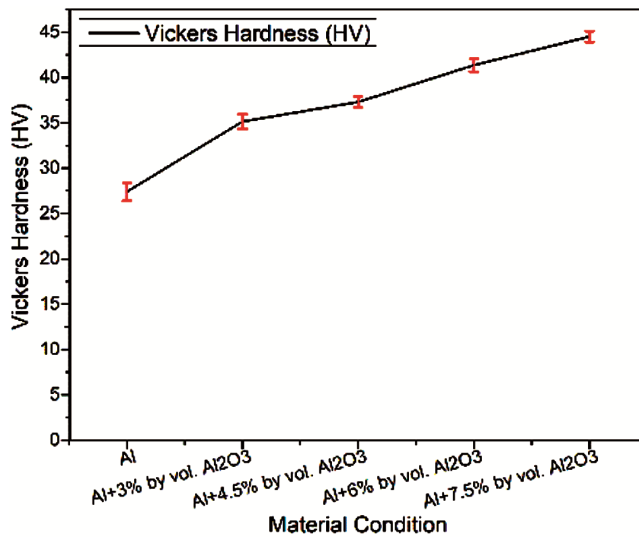


Fig. 5 — Vickers hardness (HV) values of FGM for all sample conditions.

Table 2 — Mechanical characteristics of FGM for all sample conditions

Material conditions	UTS (MPa)	YS (MPa)	Ductility (%)	Vickers hardness(HV)
Al	58	34	43	27.4
Al + 3.0% vol. Al ₂ O ₃	87	61.4	21	35.15
Al + 4.5% vol. Al ₂ O ₃	95.2	56.2	11.5	37.3
Al + 6.0% vol. Al ₂ O ₃	99	57.7	16.5	41.35
Al + 7.5% vol. Al ₂ O ₃	102.4	66	23.5	44.5

pure Al alloy while congregated Al₂O₃ particles were present in FGM samples resulting in reduced ductility of FGM samples. In addition, these deformities can infatuation the microstructural continuity of functionally graded material so that the ductility decreases significantly, as reported in the literature⁴². In this work, it is observed that reinforcement (Al₂O₃) density is higher than aluminium due to the centrifugal action of the casting⁴³. Therefore, variation in mechanical properties in thickness direction of FGM is observed. In FGM samples 4.5%vol., 6%vol. and 7.5%vol. the YS, UTS and hardness values are increased to 56.2 MPa, 95.2 MPa and 37.3 HV, 57.7 MPa, 99 MPa and 41.35 HV, and 66 MPa, 102.4 MPa and 44.5 HV respectively, while a loss in ductility value is seen as 11.5%, 16.5% and 23.5% as compared to the pure Al alloy material.

Stress-strain curve of pure Al alloy and FGM samples with various reinforcement particle compositions is shown in Fig. 4. We observed that the larger value of UTS were found in the higher vol. % Al₂O₃ specimens, due to dispersion-strength effect. Results designate that the tensile characteristics like

UTS and YS increase with the increase in Al₂O₃ content^{44, 45}. It may be mentioned that dispersion-strengthened reinforcing particles are achieved by internal oxidation, which blocks the movement of dislocation and pin-up dislocations lines. In addition, these are vital to enhancing the dislocation density in the metal matrix resulting improved values of yield and tensile strength as reported in the literature⁴³.

Figure 5 shows the variation in hardness for Al alloy and other samples of FGM having dissimilar vol. percentage of Al₂O₃. In this study, it was observed that the value of hardness has augmented with the volume percentage of reinforcing particles. In addition, a large gap in values of hardness moving from outside reinforced-zone to free particle-zone were also observed. After investigation, the observation is made that the high density of Al₂O₃ particles were more in outer-zone in comparison to inner-zone of the casted ring with owing to centrifugal force. Upon increasing the volume % of reinforcing particles, the Vickers hardness value of FGM samples increases as recorded in the Fig. 5. This is due to the postulates of the reinforcement in which Al₂O₃ particles density increases in outer zone as reported by Vieira *et al.*⁴¹. The study revealed that improvement in value of hardness of composite material is owing to the presence of composite gradient⁴⁶. It may be mentioned that gradients in the composite affects the characteristics like Young’s modulus (E) and CTE as reported by various scientists/researchers^{47, 48}. Moreover, it affects the properties characteristics like Young’s modulus and CTE same as in the present case.

3.3 Post tensile tests fracture morphology

To analyse the type of failure in samples with different compositions, fractured surface analysis is done through FESEM. The failure mode of pure Al sample and reinforced Al samples with different compositions mainly depend upon the microstructural features, type and nature of the dimpled structure, type of reinforcing particles such as Al₂O₃. Such types of features can be evidenced from Fig. 6(a)-(e). Figure. 6(a) shows the fractograph of pure Al, which reveals the presence of a higher fraction of coarser dimples dispersed in the fractured surface. This is the reason behind the large ductility of the pure Al sample. Figure 6(b) shows the fractograph for pure Al sample reinforced with 3.0% vol. Al₂O₃. It can be clearly evidenced from this Figure. that the fraction of dimpled features slightly reduced along with the brittle fracture. This mix-mode fracture causes the ductility of material to be reduced up to 21%. Fractograph corresponding to 4.5 % reinforcement is shown in Fig. 6(c). From this fractograph, it is

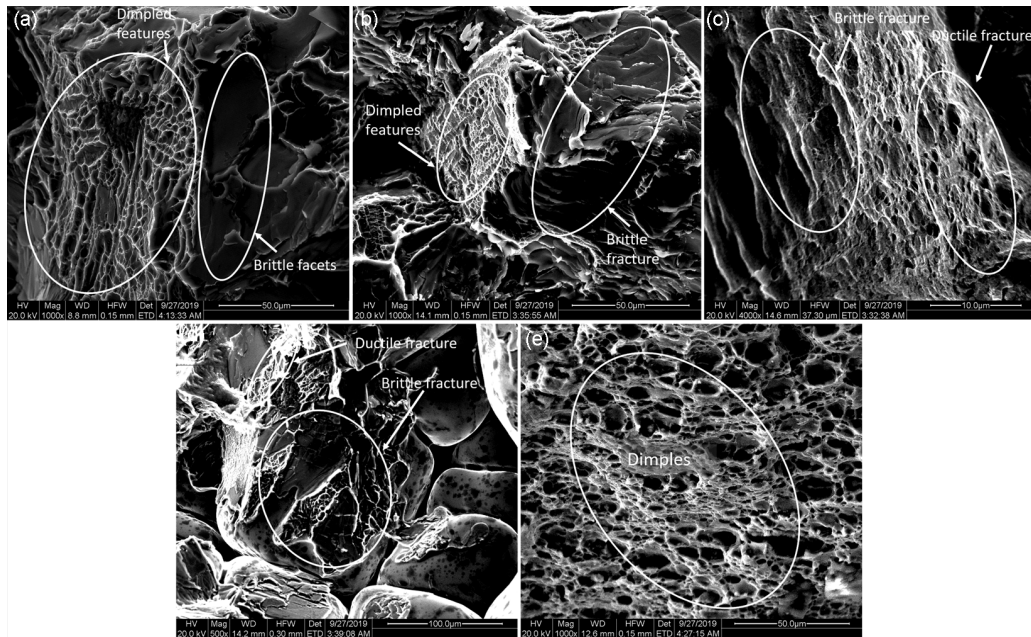


Fig. 6 — Fractographs after tensile testing, (a) pure Al-alloy, (b) FGM with 3% vol. Al_2O_3 reinforced, (c) FGM with 4.5% vol. Al_2O_3 reinforced, (d) FGM with 6% vol. Al_2O_3 reinforced, and (e) FGM with 7.5% vol. Al_2O_3 reinforced.

observed that the fraction of dimples on the surface is reduced to a significant amount and the fraction of brittle facets is observed to be more which results in the reduced ductility of the material. Further the increase in vol. % of reinforcement from 4.5% to 6% in pure Al does not improve the ductility of the material significantly which can be seen in Fig. 6(d). It might be due to the larger surface occupied by the brittle facets zone as compared to dimpled features. In addition, reinforcement is uniformly distributed in the surface (Fig. 6(c)), causing much more elongation in the previous condition. The mechanism of failure in this material condition is again the mix-mode fracture. Fig. 6(e) shows the fractograph for pure Al reinforced with 7.5% vol. Al_2O_3 . In this fractograph it can be seen clearly that the dimples are dispersed throughout the surface which evidences the improved ductility of the material w.r.t. all reinforcing conditions. In Fig. 6(e) the fine dimples are due to Mg_2Si precipitates and the coarse dimples are due to alumina particles.

3.4 Fracture toughness

In engineering application testing under monotonic load is important to check the deformation behaviour of material⁴⁹. In general, the uniaxial stress states are subjected to tensile testing specimens, while the fracture toughness testing implicates a high amount of tensile tri-axiality as reported by various researchers⁵⁰. By performing the fracture toughness tests fracture behaviour under dynamic testing in presence of an already existing crack can be obtained⁵¹⁻⁵³.

The admirable mechanical properties are shown by the centrifugally cast FGM, but deformation ability is depreciated owing to the decrement in the percentage of elongation and initiation of crack on the reinforcing particles with an increase in the percentage content of reinforcing particles.

To evaluate the studies of the parameters of fracture toughness, the specimens were prepared by following the prescribed ASTM standards⁵²⁻⁵³. Consequently, the 3-point bend (3PB) testing was implemented to find the parameters of fracture toughness of centrifugally cast functionally graded material and Al alloy using a single-edge notch bending specimen. In the present work, the notch was pre-cracked machined therefore the obtained values of fracture toughness is provisional/apparent as reported in the current work. Details regarding the sample dimension and sample preparation for 3PB testing has been discussed in the literature⁵².

Figure 7 shows the fracture toughness variation (load vs. extension curves) after 3PB testing for pure Al and FGMs samples. The apparent fracture toughness (designated as K_Q), has been measured by using the equation similar to literatures⁵³.

$$K_Q = \frac{P_Q}{B} \frac{s}{W^{\frac{3}{2}}} \left[2.9 \left(\frac{a}{W} \right)^{\frac{1}{2}} - 4.6 \left(\frac{a}{W} \right)^{\frac{3}{2}} + 21.8 \left(\frac{a}{W} \right)^{\frac{5}{2}} - 37.6 \left(\frac{a}{W} \right)^{\frac{7}{2}} + 38.7 \left(\frac{a}{W} \right)^{\frac{9}{2}} \right] \quad \dots (1)$$

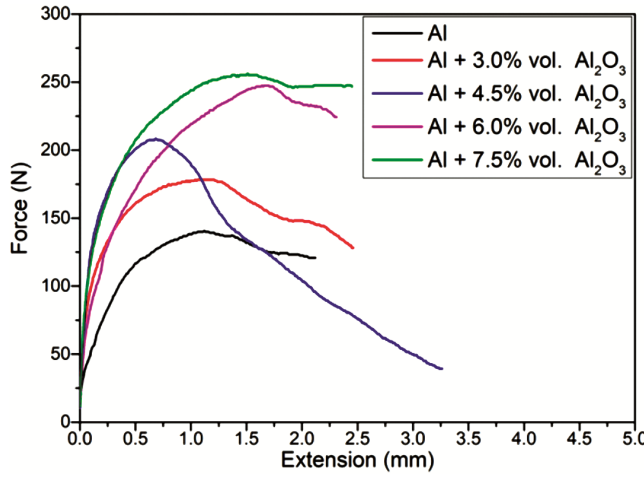


Fig. 7 — Fracture toughness results (Load vs. Extension curve) for all material conditions.

Where S = 30 mm (specimen length)

From Eq. (1) the value of K_Q is reported as the material’s plain-strain fracture toughness (K_{IC}), where crack length a, the unbroken ligament is b and specimen thickness is B. If the above validation conditions do not meet, the value of K_Q , which is found out from Eq. (1), is named as provisional/apparent fracture toughness as reported in the text^{54, 55}. But the samples prepared by the centrifugally cast product, which were having a limited thickness and size, so in the current investigation, we have reported it as a provisional fracture toughness (K_Q) of the material. In Table 3, the tabulated value shows the K_Q for pure Al-alloy which comes out as 4.62 MP \sqrt{m} and by the same procedure has been adopted to determine the various FGM samples. The values are tabulated in Table.3 and the same is shown in Fig. 8.

ASTM standard (E 992)⁵⁶ has also been used to investigate the equivalent/volumetric energy fracture toughness (K_{ee}) as one of the key parameter of fracture which is used for comparative analysis of fracture measuring parameters of pure Al and FGM at various reinforcing conditions in this work as per the following equation⁵⁷⁻⁵⁸.

$$K_{ee} = \frac{P_E S}{B W^{\frac{3}{2}}} \left[2.9 \left(\frac{a}{W} \right)^{\frac{1}{2}} - 4.6 \left(\frac{a}{W} \right)^{\frac{3}{2}} + 21.8 \left(\frac{a}{W} \right)^{\frac{5}{2}} - 37.6 \left(\frac{a}{W} \right)^{\frac{7}{2}} + 38.7 \left(\frac{a}{W} \right)^{\frac{9}{2}} \right] \dots (2)$$

In the present work pure Al has shown the least values of apparent and volumetric energy fracture toughness. On increasing the volume percent of Al₂O₃ gradual increase in the fracture toughness

Table 3 — Fracture measuring parameters of FGM for all sample conditions

Material Condition	Provisional fracture toughness (K_Q)(MPa \sqrt{m})	Volumetric energy fracture toughness (K_{ee})(MPa \sqrt{m})
Al	4.62	9.12
Al + 3.0% vol. Al ₂ O ₃	5.85	13.59
Al + 4.5% vol. Al ₂ O ₃	6.83	16.79
Al + 6.0% vol. Al ₂ O ₃	8.12	17.55
Al + 7.5% vol. Al ₂ O ₃	8.40	20.27

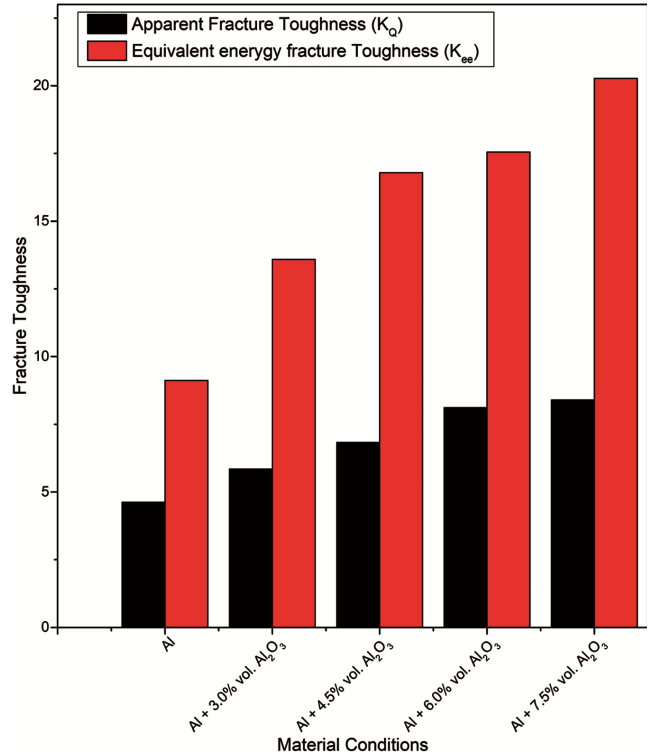


Fig. 8 — Provisional fracture toughness (K_Q) and volumetric energy fracture toughness (K_{ee}) for various material conditions.

values were observed and observed to be maximum for Al + 7.5% vol. Al₂O₃.

3.5 Post fractography of 3-point bend test

Fractured face morphology after three-point bend tests are shown in Fig. 9(a)-(e). Figure 9 (a) represent the pre-cracking zone. Figure 9(b) is the SEM photograph showing the fracture surface of pure Al. Majority of the surface in this case is perturbed with brittle facets and cracks. Fracture toughness relies upon the crack initiation and cracks propagation phase. If the crack-initiation is delayed material will have higher fracture toughness, however, if the crack propagation phase is shorter the crack will travel faster resulting in poor fracture toughness. In this case

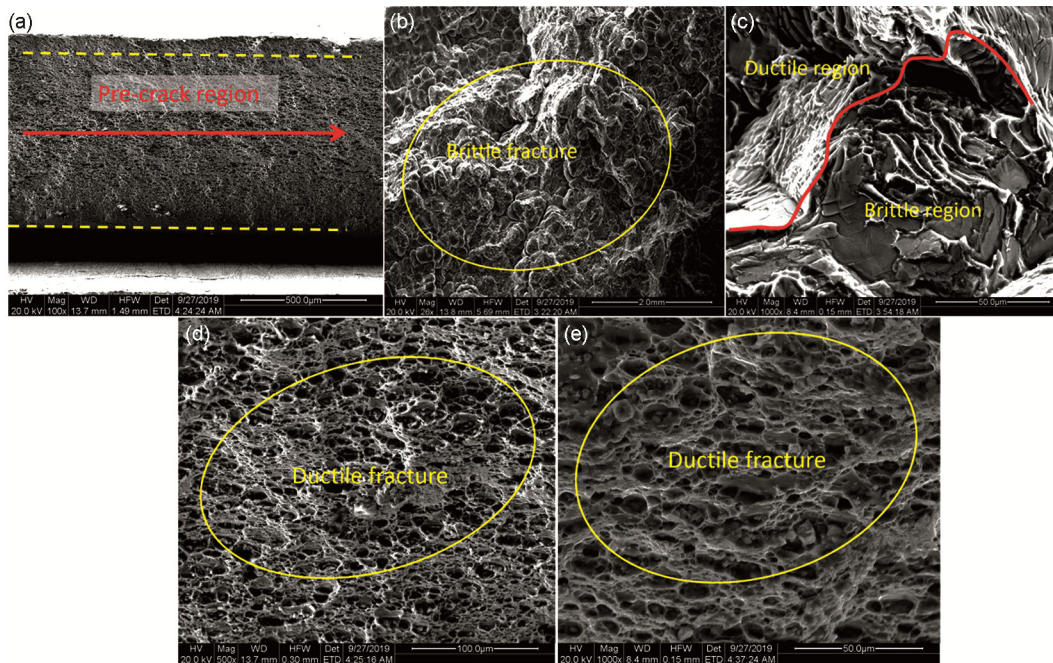


Fig. 9 — Fractographs after 3PB testing: (a) Pre-crack zone (b) Pure Al alloy, (c) FGM with 3% vol. Al_2O_3 reinforced, (d) FGM with 6% vol. Al_2O_3 reinforced, (e) FGM with 7.5% vol Al_2O_3 reinforced.

materials fracture surfaces have a larger area of brittle facets. Such type of surface may provide ease in crack movement resulting poor fracture toughness of pure Al. Fig. 9(c) shows the fractograph of pure Al reinforced with 3.0% vol. Al_2O_3 . The fractograph represents the mix-mode fracture with a higher fraction of dimpled surface, which causes the improvement in the fracture toughness parameters due to the delay in the crack propagation phase. In addition, this can be attributed to that the larger number of dimples taking a large amount of energy before the rupture. Fig. 9(d) represents the fractograph for pure Al reinforced with 6.0% vol. Al_2O_3 . The most of the region of fractured surface surrounded by ductile dimples associated with minor cracks. The coarser dimples require higher energy before rupture along with delaying in crack movement, which validates the higher value of fracture toughness parameter values for the present case. Figure 9(e) represents the fractograph for pure Al reinforced with 7.5 % vol. Al_2O_3 . The fractograph represents the higher fraction of fine dimples dispersed throughout the surface which results in the improved values of fracture toughness parameters.

4 Conclusion

In this experimental study, the FGMs were produced via a centrifugal-casting route at a uniform speed. The

microstructural and mechanical characteristics of Al/ Al_2O_3 FGM were investigated by SEM, tensile test, hardness test and fracture toughness tests. The following conclusions are drawn:

1. Due to centrifugal force, the most of Al_2O_3 particles in 7.5 % vol. Al/ Al_2O_3 FGM are enriched in the outer zone of the cast product ring, while the inner zone of the ring has a lower density of Al_2O_3 particles.
2. Mechanical characteristics of FGM have augmented with increasing the vol. % of Al_2O_3 reinforced particles at the expense of ductility due to the presence of congregated Al_2O_3 particles.
3. The fracture measuring parameters of the FGM have been observed to be higher with increasing the vol. % of Al_2O_3 due to the delay in the crack propagation phase.

References

- 1 Arunkumar S, Sundaram M S & Vigneshwara S, *Mater Today: Proc*, 33 (2020)484.
- 2 Miracle D B, *Compos Sci Technol*, 65(15-16) (2005)2526.
- 3 Saleh B, Jiang J, Ma A, Song D, Yang D & Xu, Q, *Met Mater Int.*(2019)1.
- 4 Duque N B, Melgarejo Z H,& SUHREZ O M, *Mater Charact*, 55(2)(2005)167.
- 5 Sobczak J J, & Drenchev L, *J Mater Sci Technol*, 29(4) (2013) 297.
- 6 Koizumi M F G M, *FGM activities in Japan. Compos Part B: Eng*, 28(1-2)(1997) 1.

- 7 Udupa G, Rao S S, & Gangadharan K V, *Procedia Mater Sci*, 5(2014) 1291.
- 8 Naito K, *J Mater Eng Perfor*, 25(5) (2016) 2074.
- 9 Ceschini L, & Montanari R eds, *Trans Tech Publications Ltd*, (2011)
- 10 Rajan T P D, Pillai R M, & Pai B C, *J mater Sci*, 33(14) (1998) 3491.
- 11 Verma V & Kumar B.M, *Mater Today: Proc*, 4(2)(2017) 3062.
- 12 Tevatia A & Srivastava S. K., *Indian J Eng Mater Sci*, 27(2020)348.
- 13 Panwer N & Chauhan A., *Sci Ind Res*, 77 (2018) 646-651.
- 14 Mohapatra S, Sarangi H & Mohanty U.K, *Manuf Rev*, 7(2020)26.
- 15 Canakci A, Varol T, Özkaya S & Erdemir F, *Univers J MaterSci*, 2(5) (2014)90.
- 16 Bhavar V, Kattire P, Thakare S & Singh, R. K. P, *Mater Sci Eng, Vol.* 229(2017) 012.
- 17 Tripathy A, Sarangi S K & Chaubey A K, *Int J Eng Technol*, 7(2018).
- 18 Feng K, Chen H, Xiong JI & Guo Z, *Mater Des*, 46(2013)622.
- 19 Shariat B S, Meng Q, Mahmud A S, Wu Z, Bakhtiari R, Zhang J, Motazedian F, Yang H, Rio G, Nam T H & Liu Y, *Mater Des*, 124 (2017)225.
- 20 Erdemir F, Canakci A & Varol T, *T Nonferr Metal Soc China*, 25(11)(2015) 3569.
- 21 Cuppoletti J ed, *Bo D-Books on Demand*, (2011)
- 22 Eidel'man E D & Durnev M A, *Tech Phy*, 63(11) (2018) 1615.
- 23 Naebe M & Shirvanimoghaddam K, *Appl Mater Today*, 5 (2016) pp. 223.
- 24 Chirita G, Soares D & Silva F S, *Mater Des* 29(1) (2008) 20.
- 25 Ulukoy A, Topcu M & Tasgetiren S, *Proc I Mech E Part J: J Eng Tribol*, 0(0) (2015)1.
- 26 Ramasamy M, Moorthy E S, Balasubramanian A, Kumaran P K S, Baig M B N, Alagappan S & Moorthy M, *Indian J Eng Mater Sci*, 28 (2021) 300.
- 27 El-Galy I M, Ahmed M H, *Alex Eng J*, (2017) 1.
- 28 Saadatmand M, & Aghaza deh Mohandesi J, *The Indian Inst Met- IIM*, (2014)
- 29 Guo J F, Liu J, Sun C N, Maleksaeedi S, G Bi, Tan M J, Wei, J, *Mater Sci Engg:A*, 602 (2014) 143.
- 30 Shafiei Zarghani A, Kashani Bozorg S F, & Zarei Hanzaki A, *Mater Sci Eng A*, 500 (2009) 84.
- 31 Tohgo K, Suzuki T, & Araki H, *Eng Frac Mech*, 72 (2005) 2359.
- 32 Rousseau C E, & Tippur H V, *Acta Mater*, 48(2000) 4021.
- 33 Sathiskumar R, *Mater Charact*, (2013) 84.
- 34 Lin J S & Miyamoto Y, *Acta Mater*, 48(2000) 767.
- 35 Moon R J, Hoffman M, Hilden J, Bowman K J, Trumble K P, & Rodel, J, *Eng Frac Mech*, 69(2002) 1647.
- 36 Rodriguez Castro R, Wetherhold R C, & Kelestemur M H, *Mater Sci Eng A*, 323(2002). 445.
- 37 ASTM E399-05 *American Society for Testing and Materials, Philadelphia*, (2005).
- 38 Kumar B, Mer K K S, & Prasad L, *Trends Mater Eng*, (2019) 6
- 39 Thirtha Prasad H P, Chikkanna N, *IJAET/Vol.II/ Issue IV*, (2011) 161.
- 40 Vieira A C, Sequeira P D, Gomes J.R & Rocha L A, *Wear*, 267 (2009) 585.
- 41 Mutuka T, & Gürbüz M, *Indian J Eng Mater Sci*, 27(2020), 1027.
- 42 Ulukoy A, Topcu M, & Tasgetiren S, *Chapter 5*, (2016).
- 43 Li CQ, Xu DK, Zu TT, et al. *J Magnets Alloys*, 56(2) (2015) 106.
- 44 Yu Dai, Quan yang Ma, Wei ting Liu, et al, *Mater Sci Technol*, (2017).
- 45 Bhowmik A, Dey D & Biswas A, *Indian J Eng Mater Sci*, 28 (2021)46.
- 46 Singh, S & Chauhan N R, *Indian J Eng Mater Sic*, 28 (2021) 189.
- 47 Kim D, Park K, Chang M, Joo S, Hong S, Cho S & Kwon H, *Met*(2019) 8.
- 48 Jin Z H & Batra R C, *J mech Phys Solids*, 44, 8 (1996) 1221.
- 49 Hohenwarter A, Pippen R, *Scr. Mater*, 64(2011) 982.
- 50 Hohenwarter A & Pippen R, *Mater Sci Eng, A* 527(2010) 2649.
- 51 Amit J, Yogesha K K, Nikhil K & Jayaganthan R, *Metallogr Microstruct Anal*, 5, no. 6 (2016) 540.
- 52 ASTM, E. "399-05" (2005).
- 53 Watanabe Y & Fukui Y, *Metall Mater Sci*, 4 (2000) 51.
- 54 Shaurya P, Amit J & Manoj K P, *Metallogr Microstruct Anal*, 8 no. 5 (2019): 581.
- 55 Wang Y M, Ma E, *Acta Mater*, 52(2004) 1699.
- 56 Lai M O, *Eng Fract Mech*, 27, 121 (1987)
- 57 Tochaee B, Hosseini H R M & Reihani S M S, *J Alloys Compd*, 681, 1(2016) 2, A. E992, (1984).